



OPEN Metre-scale vertical zonation of corals and sponges on a deep-marine cliff reflects trophic resource partitioning

Wilder Greenman^{1✉}, Francisco Javier Murillo², Bárbara de Moura Neves³, Ellen Kenchington², Liam Jasperse⁴, Aislinn Fox^{4,5}, Brett Walker^{4,5}, Evan Edinger⁶ & Owen Sherwood¹

Corals and sponges are considered foundational species and can create biodiversity hotspots in the deep sea, yet little is known of their competitive interactions, particularly with respect to resource partitioning among benthic fauna. Here we report on the feeding ecology of deep-water corals, sponges, ascidians, and anemones from a ~450 m deep submarine canyon wall off Nova Scotia, Canada. Analysis of bulk stable isotopes of carbon and nitrogen confirms isotopic niche partitioning between species despite their physical proximity. Compound-specific nitrogen isotopes of amino acids ($\delta^{15}\text{N-AA}$) separated the taxa along continua of trophic position and benthic-pelagic coupling and resolve the conspicuously enriched bulk nitrogen patterns commonly observed in sponges. Radiocarbon dating (as $\Delta^{14}\text{C}$) of tissue samples, particulate organic matter (POM) and dissolved inorganic carbon (DIC) from the Scotian Slope sheds light on food provenance and distinguishes diets dominated by older, recalcitrant forms of organic matter versus surface-derived POM. Our results reveal significant differences in resource utilisation among sympatric corals, sponges, ascidians, and anemones and highlight that organisms capable of feeding on more recalcitrant resources will likely play a greater role in supporting deep-water habitats where the quality and flux of fresh POM may be diminished.

Keywords Trophic ecology, Deep-water corals and sponges, Compound-specific isotope analysis, Nitrogen, Radiocarbon, Northwest Atlantic

Deep-water corals and sponges support complex habitats which provide shelter, substrate and nutrients for myriad benthic fauna and commercially important fish stocks^{1–3}. Corals and sponges are generally thought to feed on particulate (POM) and/or dissolved (DOM) organic matter reservoirs, yet we still know little about their specific source diets⁴. Moreover, climate-driven changes in marine primary productivity⁵ and biogeochemical cycles^{6,7} may alter food quantity and quality in deep-water habitats^{8,9}. A more comprehensive understanding of benthic community trophodynamics is therefore needed to help manage and conserve deep-water coral and sponge habitats.

Deep-water corals are passive suspension feeders and may consume both surface-water derived and deep suspended materials, potentially including phytodetritus, zooplankton and their faecal pellets^{10–12}. Early work suggested that many deep-water corals are opportunistic feeders^{13,14}. More recent studies suggest that coral feeding behaviour may be more selective than previously thought^{15,16}, and might include seasonal variability and/or dormancy^{11,17}. Sponges actively filter large volumes of water to extract POM and DOM^{18–20}. Recent studies propose a wide range of possible trophic positions spanning primary consumers to top predators^{21–23}, which collectively highlight the need for better tools to comprehend their complicated microbial symbioses. Diet overlap has been inferred between deep-water corals and sponges²⁴, but few studies of specimens cohabitating small areas exist to support this interpretation. In addition to niche overlap, feeding experiments demonstrate

¹Department of Earth and Environmental Sciences, Dalhousie University, Halifax, NS, Canada. ²Fisheries and Oceans Canada, Dartmouth, NS, Canada. ³Fisheries and Oceans Canada, St. John's, Newfoundland, Canada. ⁴Department of Earth and Environmental Sciences, University of Ottawa, Ottawa, ON, Canada. ⁵Department of Earth System Sciences, University of California, Irvine, Irvine, CA, USA. ⁶Department of Geography, Memorial University, St. John's, Newfoundland, Canada. ✉email: wilder.greenman@dal.ca

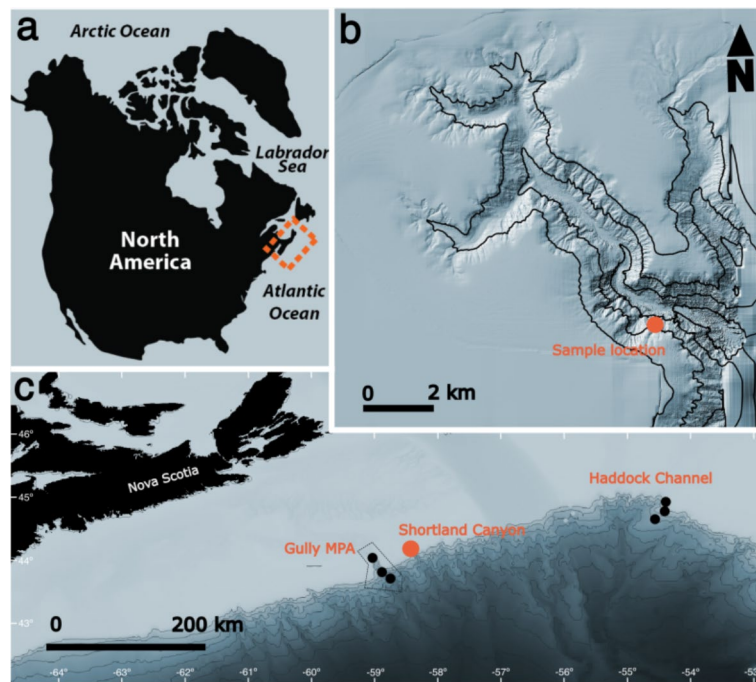


Fig. 1. Location of Shortland Canyon on the continental slope off Nova Scotia, Canada. **(a)** Inset map of North America. **(b)** Multi-beam imagery of Shortland Canyon showing sample location and contour lines at 200 m intervals. **(c)** Nova Scotia shelf and slope highlighting location of Shortland Canyon. Black dots in Gully Marine Protected Area (MPA) and Haddock Channel mark DIC/POM sampling locations. Contour lines at 500 m intervals. Multibeam imagery of Shortland Canyon from the Geological Survey of Canada²⁹ and modified using QGIS version 3.40.1.

that corals are capable of consuming recycled sponge-derived material²⁵ and that sponges can assimilate mucus secreted from corals^{21,26}. The difficulty of accessing deep-water habitats and the resulting scarcity of observational feeding data for cohabiting corals and sponges severely limit our ability to expand and generalize on these interpretations.

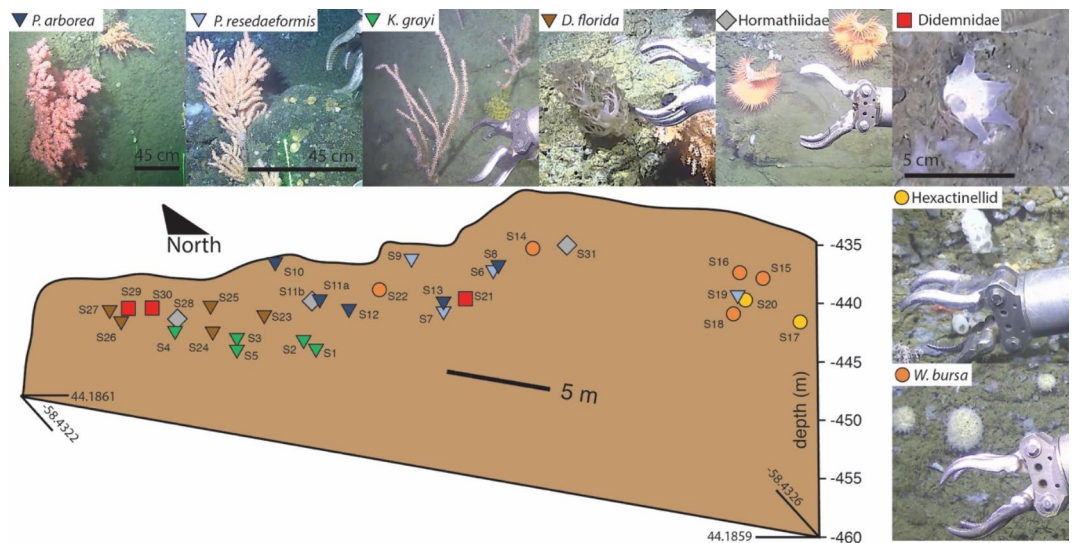


Fig. 2. Distribution of faunal samples collected along a 35 m wide vertical wall transect within Shortland Canyon. Lower corners of the plot show latitude and longitude. Symbols and colours used to represent taxa are consistent throughout the rest of this article. Manipulator hand is ~20 cm long. See supplemental videos for more detailed distribution patterns.

In 2022, we visited the upper continental slope off Nova Scotia (Eastern Canada) to investigate deep-water coral and sponge habitats using a remotely operated vehicle (ROV; Fig. 1). In this region, incised canyons host rich assemblages of corals and sponges along steep to vertical ridge walls^{27,28}. We collected specimens from a vertical wall within Shortland Canyon at a depth of 438–454 m over a 35 m wide transect (Fig. 2; supplemental videos). Octocorals of the order Scleractyonacea were observed to exhibit a conspicuous vertical zonation, with dense stands of *Paragorgia arborea* located along ridge crests, and *Primnoa resedaeformis* located directly below. More sparsely distributed *Keratoisis grayi* were located toward the ridge bases. Sampling also included Malacalcyonacea corals (*Duva florida*), sea anemones (Hormathiidae), sponges (*Weberella bursa*, and an unidentified Hexactinellid), and ascidians (Didemnidae), which were distributed with less apparent vertical zonation. This setting provided an unparalleled opportunity to investigate trophic resource partitioning among primary and secondary consumers where food availability and local hydrodynamics should be relatively equal.

We use bulk and compound-specific stable isotopes to test whether resource partitioning exists between species of corals, sponges, ascidians, and anemones living metres apart. Bulk stable carbon ($\delta^{13}\text{C}_{\text{bulk}}$) and nitrogen ($\delta^{15}\text{N}_{\text{bulk}}$) isotopes were used to assess differences in resource utilization. Compound-specific nitrogen isotope analysis of amino acids ($\delta^{15}\text{N}_{\text{AA}}$) was used to further differentiate taxon-specific diets by baseline sources, trophic position, and microbial resynthesis. We also compare radiocarbon ($\Delta^{14}\text{C}$) of tissue samples with a new dissolved inorganic carbon (DIC) depth profile and mixed layer suspended POM (POM_{susp}) from the Scotian Slope to elucidate food provenance.

Results and discussion

Bulk stable isotopes reveal significant trophic niche partitioning

When plotted in $\delta^{13}\text{C}_{\text{bulk}}$ vs. $\delta^{15}\text{N}_{\text{bulk}}$ space, the POM_{susp} and taxa formed a positive linear relationship (Fig. 3). POM_{susp} had the lowest isotopic values ($\delta^{13}\text{C}_{\text{bulk}} = -26.4$ – -24.1 ‰; $\delta^{15}\text{N}_{\text{bulk}} = 2.7$ – 4.1 ‰). Corals *P. arborea* and *P. resedaeformis* had the next lowest isotopic values (-23.3 – -20.2 ‰; 7.3 – 9.1 ‰). Corals *K. grayi* and *D. florida*, anemones and ascidians had intermediate values (-22.6 – -20.0 ‰; 7.6 – 12.5 ‰). Sponges (Hexactinellid and *W. bursa*) had the most enriched values (-21.2 – -19.7 ‰; 13.6 – 17.6 ‰).

Conventional interpretations of the bulk isotope data in Fig. 3 would ascribe a mostly pelagic, low trophic position to taxa with lower $\delta^{13}\text{C}_{\text{bulk}}$ and $\delta^{15}\text{N}_{\text{bulk}}$ (*P. resedaeformis*, *P. arborea*) and a more benthic, high trophic position to taxa with higher $\delta^{13}\text{C}_{\text{bulk}}$ and $\delta^{15}\text{N}_{\text{bulk}}$ (sponges)^{30,31}. Strikingly, the total range of values in our assumed primary and secondary consumers ($\delta^{13}\text{C}_{\text{bulk}} = -23.3$ – -19.7 ‰; $\delta^{15}\text{N}_{\text{bulk}} = 7.3$ – 17.6 ‰) overlaps with reported ranges across virtually all trophic guilds of offshore marine ecosystems, from zooplankton to piscivorous fish, seabirds, and top predators^{31–33}. In fact, the exceptionally high $\delta^{15}\text{N}$ values in *W. bursa* approach those of polar bears when variations in baseline nitrogen are accounted for³². Traditional $\delta^{15}\text{N}_{\text{bulk}}$ -based calculations of trophic

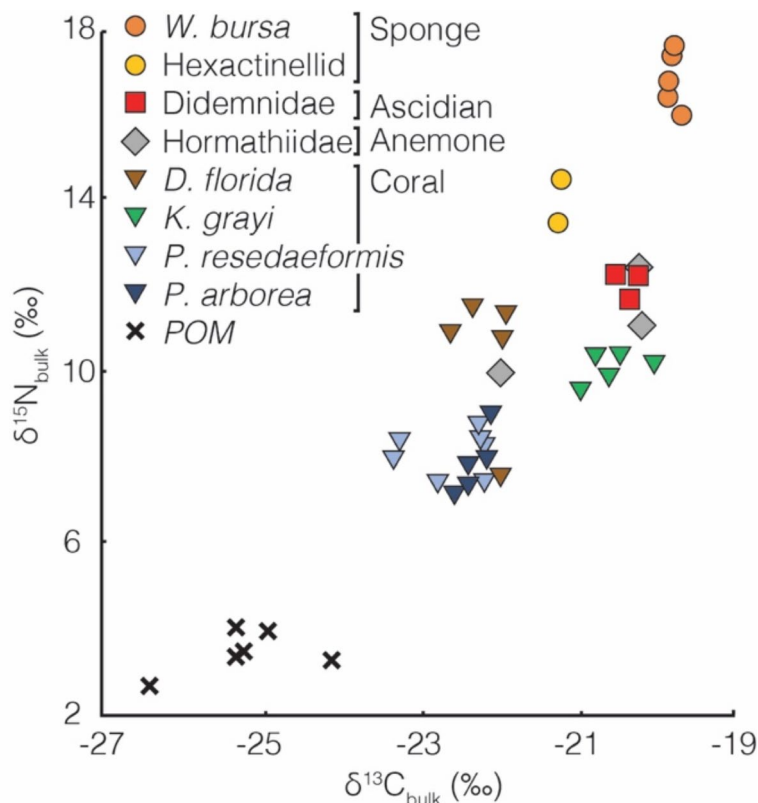


Fig. 3. Distribution of $\delta^{13}\text{C}_{\text{bulk}}$ vs. $\delta^{15}\text{N}_{\text{bulk}}$ data for specimens collected at Shortland Canyon wall transect and POM_{susp} (Gully MPA and Haddock Channel, Fig. 1).

position (TP) using POM_{susp} for the baseline $\delta^{15}\text{N}$ and a trophic enrichment factor of 3.4³¹ would suggest a range of TPs from 3.4 (*P. resedaeformis*, *P. arborea*) to 6.0 (*W. bursa*), which is unrealistic. Nevertheless, given that all taxa were contemporaneously sampled from the same cliff face, their separation in $\delta^{13}\text{C}_{\text{bulk}}$ vs. $\delta^{15}\text{N}_{\text{bulk}}$ space likely signifies actual differences in resource utilization³⁴, which we assessed further through compound-specific isotope analysis of amino acids.

Compound-specific isotope analysis of amino acids (CSIA-AA)

Analysis of $\delta^{15}\text{N}_{\text{AA}}$ was used to deconvolve factors influencing the observed wide range of $\delta^{15}\text{N}_{\text{bulk}}$. A strong positive correlation (linear regression: $r^2 = 0.68$) between $\delta^{15}\text{N}_{\text{bulk}}$ and the $\delta^{15}\text{N}$ of total hydrolysable amino acids ($\delta^{15}\text{N}_{\text{THAA}}$) confirmed that $\delta^{15}\text{N}_{\text{bulk}}$ represents the isotopic mass balance of individual amino acids. The overall distribution of $\delta^{15}\text{N}_{\text{AA}}$ data (Fig. 4) was typical of heterotrophic consumers, with relatively lower values for “source” amino acids (Src-AAs; e.g., phenylalanine; Phe) and higher values for “trophic” amino acids (Tr-AAs; e.g., glutamic acid; Glx)³⁵. Src-AAs undergo minimal isotopic fractionation in animal metabolism and therefore retain baseline $\delta^{15}\text{N}$ signatures of primary producer biomass through successive trophic levels. Tr-AAs undergo rate-limiting transamination reactions in animal metabolism, leading to stepwise enrichment of $\delta^{15}\text{N}_{\text{AA}}$ values by as much as 7 ‰ with each trophic transfer^{36–38}. In addition, microbial metabolisms may alter the distribution of $\delta^{15}\text{N}_{\text{AA}}$ values through various pathways³⁵. One such pathway is AA-selective heterotrophic resynthesis, which results in a scattering in the $\delta^{15}\text{N}$ of Tr-AAs³⁹; another pathway is extracellular hydrolysis, which leads to uniform enrichment of all AAs^{40,41}.

The $\delta^{15}\text{N}_{\text{Phe}}$ proxy for baseline $\delta^{15}\text{N}$ clearly separates corals and anemones from sponges and ascidians. For corals and anemones, $\delta^{15}\text{N}_{\text{Phe}}$ clustered tightly around a value of 5.9 ± 0.4 ‰. This value is slightly higher than the $\delta^{15}\text{N}$ of mixed layer POM_{susp} collected during August 2022 (Table 1), but within range of spatio-temporally averaged POM_{susp} and nitricline nitrate in the study region⁴². This is strong evidence that the diets for these taxa

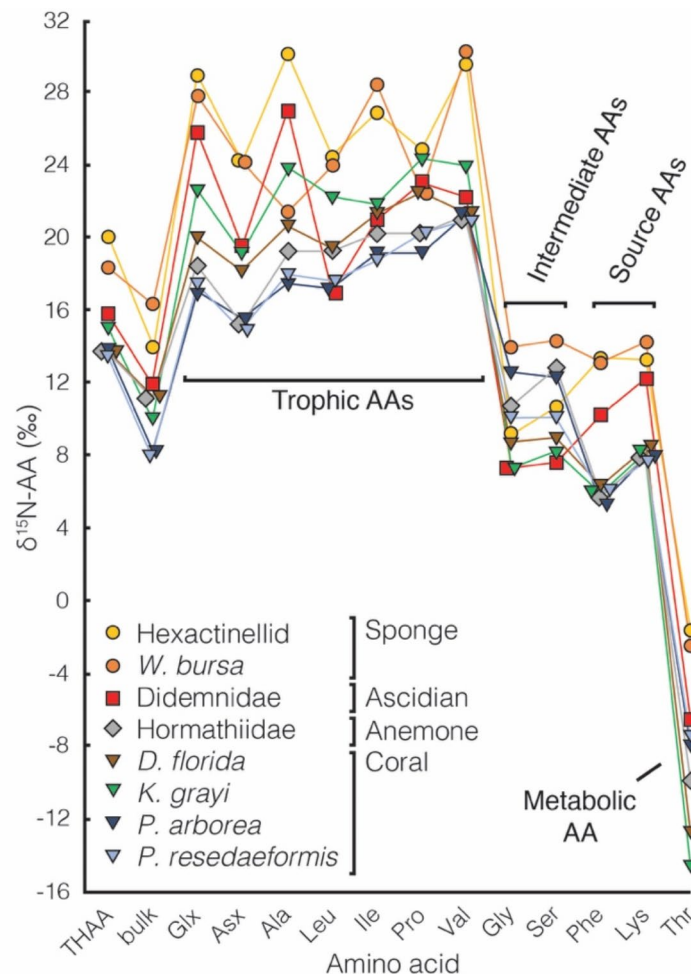


Fig. 4. $\delta^{15}\text{N}_{\text{AA}}$ results divided into trophic, intermediate, source and metabolic groupings based on established fractionation patterns^{35,36,38}. Abbreviations: Total hydrolysable amino acids (THAA), glutamic acid (Glx), aspartic acid (Asx), alanine (Ala), leucine (Leu), isoleucine (Ile), proline (Pro), valine (Val), glycine (Gly), serine (Ser), phenylalanine (Phe), lysine (Lys), threonine (Thr). Connecting lines are shown to help visualize different patterns among species.

Sample	$\Delta^{14}\text{C} \text{ ‰}$	^{14}C Age	$\delta^{13}\text{C}_{\text{bulk}}$	$\delta^{15}\text{N}_{\text{bulk}}$	$\delta^{15}\text{N}_{\text{THAA}}$	$\delta^{15}\text{N}_{\text{Phe}}$	TP_{met}	TP_{prot}	ΣV
Hormathiidae	12.1 ± 1.6	modern	-20.4	11.2	13.9 ± 1.1	5.6 ± 0.7	2.6 ± 0.1	3.3 ± 0.5	1.4 ± 0.1
<i>Duva florida</i>	8.9 ± 1.9	modern	-22.1	10.5	14 ± 0.5	6.4 ± 0.1	2.7 ± 0.1	3.5 ± 0.3	1.2 ± 0.1
<i>Keratois grayi</i>	15.2 ± 1.7	modern	-20.5	10.1	15.1 ± 0.4	5.8 ± 0.5	3.2 ± 0.1	4.3 ± 0.1	1.3 ± 0.1
<i>Paragorgia arborea</i>	16.5 ± 1.5	modern	-22.3	8.0	13.9 ± 1.1	5.4 ± 0.8	2.4 ± 0.3	3.0 ± 0.5	1.5 ± 0.2
<i>Primnoa resedaeformis</i>	13.8 ± 1.7	modern	-22.6	8.0	13.5 ± 0.2	6.1 ± 0.6	2.3 ± 0.1	2.9 ± 0.1	1.5 ± 0.1
<i>Weberella bursa</i>	7.7 ± 1.5	modern	-19.8	16.9	18.5 ± 0.1	13.2 ± 0.2	2.8 ± 0.1	2.1 ± 0.2	2.8 ± 0.1
Hexactinellid	-75.5 ± 1.8	560 \pm 12	-21.2	14.1	20.2 ± 0.2	13.5 ± 0.2	3.0 ± 0	4.0 ± 0.2	2.2 ± 0.2
Didemnidae	7.7 ± 1.5	modern	-20.4	12.1	16.0 ± 0.3	10.4 ± 0.3	3.0 ± 0.1	4.0 ± 0.2	2.7 ± 0.1
POM	0.6 ± 5.2	modern	-25.2	3.5					

Table 1. Summary table of radiocarbon, bulk carbon and nitrogen isotopes and CSIA-measured parameters of collected specimens and POM_{susp}. POM taken from a depth of 20 m. Further detail on radiocarbon data in SI.

originate ultimately from mixed layer primary production. In sponges, $\delta^{15}\text{N}$ was substantially enriched across all AAs, including Phe ($13.4 \pm 0.2 \text{ ‰}$). This pattern of enrichment indicates that the diets of sponges may be influenced by extracellular hydrolysis^{40,41} and implies that they exploit an entirely different basal food web from corals and anemones. Ascidians showed intermediate levels of $\delta^{15}\text{N}$ enrichment across most AAs, implying a different or mixed diet between that of corals and sponges.

The difference in $\delta^{15}\text{N}$ between Glx and Phe provides an internally normalised index of metazoan trophic position (TP_{met} ³⁷; see Methods). Calculated TP_{met} among all taxa ranged from 2.3 to 3.2, consistent with feeding at primary to secondary consumer levels (Table 1). An alternative formulation for TP based on the $\delta^{15}\text{N}$ difference between alanine (Ala) and Phe accounts for additional trophic steps induced by protozoan heterotrophy (TP_{prot} ⁴³; Methods). For all taxa except *W. bursa*, calculated TP_{prot} was higher than TP_{met} by 0.6–1.1 units (Table 1), indicating that protozoan heterotrophy added about one trophic level in the diets of most taxa. In *W. bursa*, TP_{prot} was lower than TP_{met} by 0.7 units. In addition, the $\delta^{15}\text{N}$ of threonine (Thr) normalized to $\delta^{15}\text{N}$ of Phe became more negative with increasing TP for corals and anemones (Fig. 4). This pattern is consistent with inverse trophic fractionation of Thr³⁸ and adds further support for separation of taxa by trophic level.

In addition to the effects of baseline $\delta^{15}\text{N}$ and heterotrophic fractionation, the distributions of $\delta^{15}\text{N}_{\text{AA}}$ exhibit differences relating to AA-selective heterotrophic microbial resynthesis, which is quantified by the ΣV parameter (Methods). ΣV provides a relative index of diet “freshness”. In corals and anemones, ΣV clustered around 1.4 ± 0.1 (Table 1). These values are typical of fresh algae and zooplankton biomass^{39,44}. In sponges and ascidians, ΣV clustered around 2.6 ± 0.3 . Such high values of ΣV are characteristic of highly degraded materials including meso- and bathy-pelagic POM_{susp}^{39,45} and DOM⁴¹. These distinct groups of ΣV values further support the inference of at least two distinct basal food webs.

$\Delta^{14}\text{C}$ values of tissue samples differentiate DOM from POM in diet composition

Food provenance was also investigated by comparing $\Delta^{14}\text{C}$ from tissue samples to a new $\Delta^{14}\text{C}_{\text{DIC}}$ depth profile collected from the upper slope region off Nova Scotia (Fig. 5). The $\Delta^{14}\text{C}_{\text{DIC}}$ profile, which peaks at $+20 \text{ ‰}$ from 150 to 200 m depth and decreases to -10 ‰ below that, reflects the uptake and subsequent mixing and dilution of atmospheric nuclear bomb-produced ^{14}C ⁴⁶. POM_{susp} was also sampled at the depth of maximum primary productivity ($0.6 \pm 5.2 \text{ ‰}$) and was lower than that of DIC, which may be explained by temporal offsets in the integration of $\Delta^{14}\text{C}$ between these two pools at the time of sampling. The $\Delta^{14}\text{C}$ value of deeper POM_{susp} and dissolved organic material (DOM) was not measured in the present study, but in northwest Atlantic slope waters these pools typically have far more negative $\Delta^{14}\text{C}$ (POM_{susp}: $< -50 \text{ ‰}$; DOM: $< -350 \text{ ‰}$ ⁴⁶). All the taxa except for Hexactinellid sponges had positive $\Delta^{14}\text{C}$ values (Table 1), confirming that their diets originate from the surface mixed layer¹⁰ (Fig. 5). Potential routes for transporting these mixed layer $\Delta^{14}\text{C}$ signals to depth include passive sinking of phytodetritus and other particulates; vertically migrating zooplankton; or downward tidal pumping^{47,48}. $\Delta^{14}\text{C}$ values of corals and anemones (avg. $+13.3 \text{ ‰}$) were slightly higher than that of ascidians and *W. bursa* (avg. 7.7 ‰), possibly reflecting zonation of food sources in the upper vs. lower part of the mixed layer, respectively⁴⁹. Alternatively, ascidians and *W. bursa* may record a mixed diet comprising both mixed layer and deeper ^{14}C -depleted food sources. Hexactinellid sponges had a remarkably low $\Delta^{14}\text{C}$ value of -75.5 ‰ (^{14}C age = 560 ± 12 years) more consistent with the $\Delta^{14}\text{C}$ of deep POM_{susp} or DOM.

To summarize, the $\delta^{15}\text{N}_{\text{AA}}$ data demonstrate that: (1) Based on TP_{met} values, all taxa feed at the level of primary to secondary consumers; (2) Higher relative values of TP_{prot} indicate that protozoan heterotrophy is an important component of the underlying food web in all diets, except for *W. bursa*; (3) Based on differences in isotopic baseline ($\delta^{15}\text{N}_{\text{Phe}}$) and microbial resynthesis (ΣV), corals and anemones rely on relatively fresh materials derived from mixed layer primary productivity, while sponges and ascidians exploit highly microbially degraded food sources; (4) Radiocarbon data confirm that the diets of all taxa, except Hexactinellid sponges, ultimately originate from the surface mixed layer.

Taxon-specific trophic niches

To further explore potential resource partitioning, isotopic metrics (except $\Delta^{14}\text{C}$ because only one sample per taxon was measured) were analysed by principal component analysis (PCA; Fig. 6). Unlike conventional

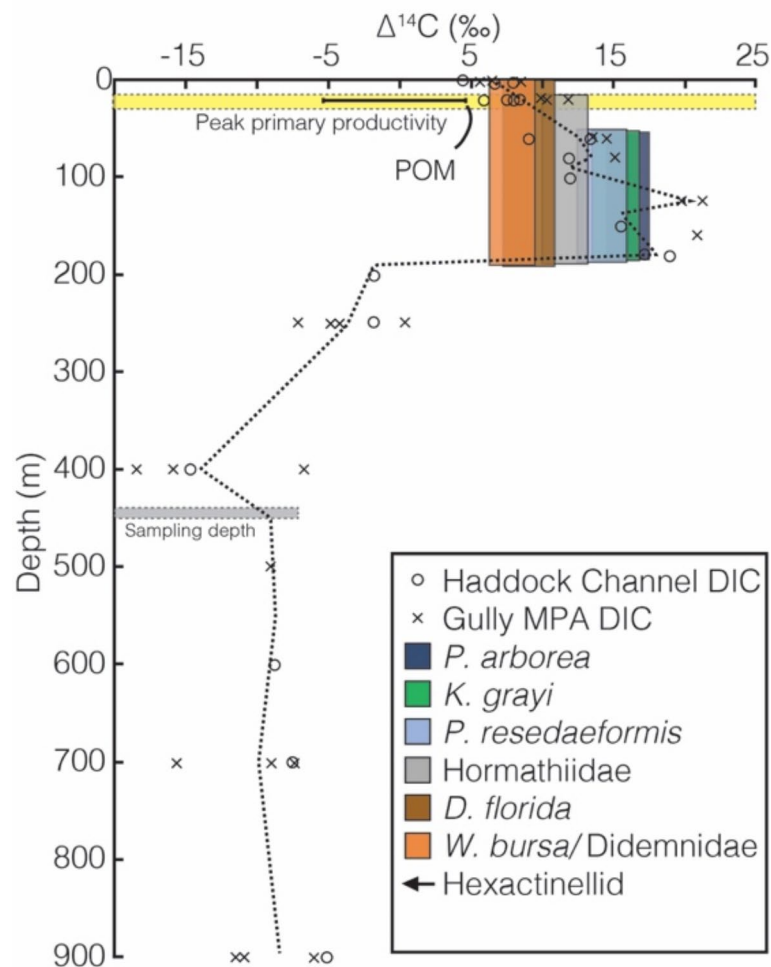


Fig. 5. Comparison between $\Delta^{14}\text{C}$ from seawater DIC and POM, and from faunal tissues. Values for DIC are from three stations in each of the Gully MPA and the Haddock Channel; black dashed line represents a composite depth profile fitted through all points. Values for POM are from the same stations, collected at the depth of peak primary productivity (~ 20 m) based on in situ O_2 profiles measured during CTD downcasts. Taxa were collected at depths of 438 to 454 m, but their tissue $\Delta^{14}\text{C}$ values are mapped to the corresponding depths on the composite profile of DIC $\Delta^{14}\text{C}$ to infer the depth at which their food sources originated.

interpretations of isotopic niches in two-dimensional $\delta^{15}\text{N}_{\text{bulk}}$ vs. $\delta^{13}\text{C}_{\text{bulk}}$ space, the separation of multiple isotopic metrics in PCA space deconvolves factors influencing $\delta^{15}\text{N}_{\text{bulk}}$ (i.e., baseline isotopic variability, trophic processing, and microbial degradation pathways) independently of each other. Because of this, the relative positions of taxa in PCA space are notably different than in Fig. 3. The first PC separated the taxa mainly along continua of $\delta^{13}\text{C}_{\text{bulk}}$, $\delta^{15}\text{N}_{\text{bulk}}$, $\delta^{15}\text{N}_{\text{Phe}}$, and ΣV . Lower values of each loading are more closely representative of diets derived from surface primary productivity, and higher values represent a decoupling via microbial processing; therefore, this axis represents an index of benthic-pelagic coupling. The second PC separates taxa mainly according to trophic level. Within this framework, corals and anemones are separated from sponges and ascidians according to benthic-pelagic coupling, while the taxa within each of these groups are separated according to trophic level. Accordingly, and with important caveats noted below, the separation of taxa in multi-dimensional PCA space strongly supports significant resource partitioning among the taxa, likely reflecting actual differences in trophic niches.

Based on the distribution of data in PCA space along with the surface-derived $\Delta^{14}\text{C}$ signatures, *P. arborea* and *P. resedaeformis* occupy a similar trophic niche, with tight benthic-pelagic coupling (mean $\delta^{15}\text{N}_{\text{Phe}} = 5.8 \pm 0.7$; $\Sigma\text{V} = 1.5 \pm 0.2$) and low trophic position ($\text{TP}_{\text{met}} = 2.3 \pm 0.2$; $\text{TP}_{\text{prot}} = 3.0 \pm 0.3$). The most probable food sources for both taxa include recently exported phytodetritus and protozoa. Fan-shaped colonies of *P. arborea* sat atop ridge crests oriented perpendicular to fast moving currents (based on ROV footage), which may optimise capture of fresher, non- or weakly motile particles^{27,50}. This positioning is consistent with in situ time lapse photography showing that feeding cycles in *P. arborea* are tightly coupled to periods of maximum flow of the diurnal tidal cycle directly above the colonies⁵¹. Bushier colonies of *P. resedaeformis* were located directly below *P. arborea*, protruding a shorter distance from the cliff face, in what presumably would be a marginally slower hydrodynamic regime. Therefore, the different vertical positions and morphologies of *P. arborea* and *P. resedaeformis* may reflect

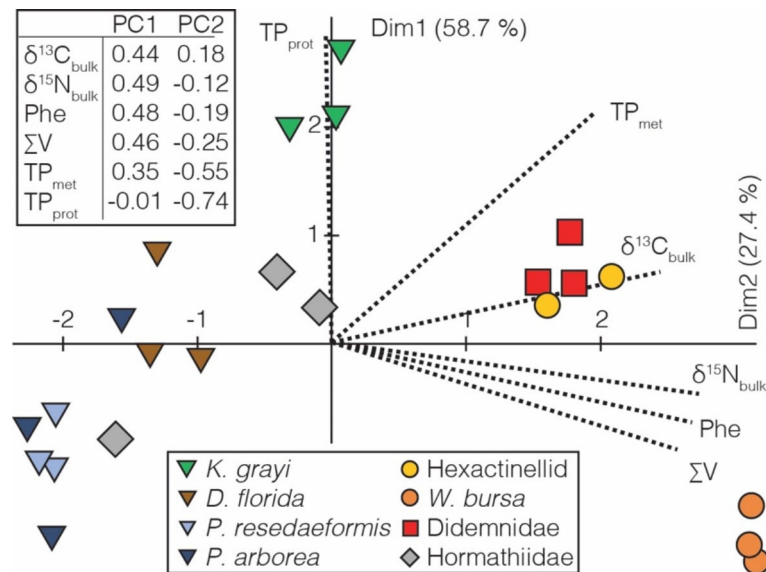


Fig. 6. Taxon-specific niche separation identified through principal component analysis (PCA) of bulk carbon ($\delta^{13}\text{C}_{\text{bulk}}$) and nitrogen ($\delta^{15}\text{N}_{\text{bulk}}$) isotopes and CSIA-based parameters including $\delta^{15}\text{N}$ of metazoan (TP_{met}) and protistan (TP_{prot}) trophic positions, baseline $\delta^{15}\text{N}$ ($\delta^{15}\text{N}_{\text{Phe}}$) and microbial resynthesis (ΣV). The two axes explain 86.1 % of the variance within the dataset.

preferential colonization of areas where the hydrodynamic regime suits the morphology of the coral to optimize nutrient acquisition⁵². Alternatively, their positioning may reflect differences in larval settlement⁵³ rather than dietary selectivity.

Keratois grayi occupied a distinct niche with the highest TP of all the taxa ($\text{TP}_{\text{met}} = 3.2 \pm 0.1$; $\text{TP}_{\text{prot}} = 4.3 \pm 0.1$) while maintaining a high degree of benthic-pelagic coupling as evidenced by the low ΣV value (1.3 ± 0.1) and similar baseline ($\delta^{15}\text{N}_{\text{Phe}}$ and $\delta^{13}\text{C}_{\text{bulk}}$) characteristics as *P. arborea* and *P. resedaeformis*. These results support previous interpretations that *K. grayi* consumes zooplankton^{16,49}. *Keratois grayi* has a spindly morphology and was observed in the lower, more sparsely populated and hydrodynamically protected part of cliff faces. It is unclear whether and how this vertical positioning might facilitate capture of motile zooplankton prey unless *K. grayi* feeding is optimized at slower current speeds⁵². Collectively, our results mirror feeding experiments where corals efficiently capture phytoplankton at higher current speeds, but preferentially prey on zooplankton at lower speeds⁵⁴. Thus, even in such a confined sampling area, meter-scale variability in hydrodynamic patterns appears to be tied to complementary morphological traits, supporting that feeding behaviour of corals is inextricably linked to morphology and flow at metre-scale resolution⁵². These results shed light on the drivers of localized species distribution segregation commonly observed in deep-water benthic vertical wall communities^{55,56}.

Malacalcyonacean soft corals (*D. florida*) and anemones (Hormathiidae) occupied a region in PCA space between that of *P. arborea*/*P. resedaeformis* and *K. grayi*, based on intermediate values of TP_{met} (avg. 2.8) while maintaining a high degree of benthic-pelagic coupling (Fig. 6; Table 1). Low ΣV values in *D. florida* (1.2) and Hormathiidae (1.4) may support a high proportion of live prey consumption (Table 1). In contrast to larger octocorals, the seemingly more random spatial distribution of soft corals and hemisessile nature of anemones (Fig. 2) may decouple their feeding strategy from local hydrodynamics. These characteristics imply opportunistic feeding of relatively fresh food sources for soft corals and anemones, consistent with observed feeding in shallow and deep-water counterparts⁵⁷. At Shortland Canyon, their diets likely comprise smaller zooplankton prey such as foraminifera, amphipods, and invertebrate larvae⁵⁸. Our results support previous observations that Malacalcyonacean corals are niche generalists in the northwest Atlantic⁵⁹. For anemones, feeding based on CSIA-AA proxies appears less carnivorous than generally recognized⁶⁰.

Sponges and ascidians exploit a different basal food web characterised by a high degree of microbial reprocessing. The high values of ΣV (mean = 2.6 ± 0.2) and baseline $\delta^{15}\text{N}_{\text{Phe}}$ (12.4 ± 0.4) suggest that both selective heterotrophic resynthesis and extracellular hydrolysis may play important resource utilisation roles for these taxa. The $\delta^{15}\text{N}_{\text{AA}}$ enrichment patterns in sponges and ascidians resembles the few existing measurements of $\delta^{15}\text{N}_{\text{AA}}$ in mesopelagic suspended POM^{40,41}. For Hexactinellid sponges, the additional constraint of pre-bomb $\Delta^{14}\text{C}$ strongly indicates that these sponges feed on a fraction of pre-aged, hydrolytically degraded, suspended POM and DOM. *Weberella bursa* and ascidians, however, had distinct post-bomb $\Delta^{14}\text{C}$ signatures, implying that neither deep POM_{susp} or DOM are proximate food sources for these taxa. Rather, the enzymatic hydrolysis responsible for the elevated $\delta^{15}\text{N}_{\text{AA}}$ patterns in these taxa may happen internally within their holobionts^{22,61,62}. Despite these uncertainties, the data clearly support additional trophic niche partitioning even among morphologically similar sponges and ascidians.

Combined, bulk stable carbon ($\delta^{13}\text{C}_{\text{bulk}}$) and nitrogen ($\delta^{15}\text{N}_{\text{bulk}}$), $\delta^{15}\text{N}_{\text{AA}}$ and ^{14}C data capture a wide separation in resource utilisation among deep-water benthic fauna living only metres apart. Our multifaceted approach explains anomalously elevated $\delta^{15}\text{N}_{\text{bulk}}$ values commonly observed in sponges^{22,23,30,63,64} as due

to baseline nitrogen and microbial reprocessing. The spatially constrained sampling location standardised many environmental aspects, but factors such as tissue turnover rates, isotopic fractionation associated with starvation, fasting or reproduction, recruitment strategies and microbiome-specific metabolic processes are challenging to constrain through isotopic proxies. In addition, the potential impact of ecological interactions and specific anatomic peculiarities could not be assessed. Isotopic proxies of tissue samples record time-averaged feeding preferences, but seasonal changes such as winter dormancy as observed in *P. arborea*¹⁷, may preserve a bias towards high productivity months. While the parameters we measured do not fully encompass individual trophic niches, our results reveal significant differences in resource utilisation among functionally similar taxa, which collectively increase community level nutrient acquisition and support niche complementarity⁶⁵ rather than competition.

Implications for broader species distribution patterns of coral and sponge habitats

Vertical zonation patterns at the sampling location were also seen at other cliff faces in Shortland Canyon and the Gully Marine Protected Area (MPA) during the 2022 and earlier expeditions²⁸. Interestingly, these meter-scale zonation patterns reflect broader bathymetric distributions long recognized by fishermen⁶⁶ and documented in bycatch records and targeted surveys^{67–69}. For example, along the eastern Scotian slope, *P. resedaeformis* and *P. arborea* are concentrated within a relatively shallow and narrow range of water depths (230–500 m), *K. grayi* occurs deeper (350–900 m), while Polymastiidae (including *W. bursa*) and Hexactinellid sponges have wider depth tolerances (190–915 m)⁷⁰. Because environmental factors such as temperature, salinity, seawater chemistry, slope (as a proxy for substrate) and current regime tend to co-vary with depth, it has remained unclear which factors are limiting to taxon distributions^{70,71}. In the present study, all these environmental factors except for current regime should be constant along the cliff face. Currents on the other hand would be expected to vary on the cliff face with vertical position, aspect, and physical obstacles. Thus, we hypothesize that current regime and its influence on food availability and utilization must play a first order constraint on overall taxon-specific depth distributions. If true, then the taxa studied here should exhibit similar patterns of resource utilization over their broader depth distributions.

Nutrient recycling pathways in deep-water coral and sponge habitats

Global shifts in plankton biomass and community composition^{5,72} pose poorly constrained threats to deep-water coral and sponge habitats⁹. Where POM flux is negatively impacted, sponges may add resilience to their habitats by consuming DOM and supplying POM to neighbouring fauna via predation or detritovory (i.e. the sponge loop)^{73,74}. Our results support that sponges and ascidians do not demonstrate strong benthic-pelagic coupling, and exploit recalcitrant, microbially degraded food sources. In particular, Hexactinellids are completely decoupled from surface primary productivity because they feed on DOM and deep POM_{susp}. While our study does not include predators, similar food web studies using CSIA parameters observe that taxa one trophic guild above sponges (i.e. sea stars, sea urchins, and anemones) have similarly high ΣV values²². This may hint that sponge-derived food sources are commonly used by neighbouring organisms. These results support the use of CSIA-AA for recognizing specific nutrient recycling pathways in natural environments. The ability of deep-marine benthic communities to recycle recalcitrant sources of organic matter will be critical in regions experiencing long-term food shortages due to decreased nutrient export from the surface ocean.

Methods

Collection of biological samples

Sampling was conducted during an expedition aboard the M/V *Atlantic Condor* with a remotely operated vehicle (ROV) in August 2022. Biological specimens were collected from a single cliff face at Shortland Canyon (44°11'9.64"N, 58°25'56.64"W) at depths of 438–454 m. Five specimens each of corals (*P. arborea*, *P. resedaeformis*, *K. grayi*, *D. florida*) and demosponges (*W. bursa*), three anemones (Hormathiidae), two unidentified hexactinellid sponges (same morphotype), and three ascidians (Didemnidae) were collected. The challenges of maintaining ROV position in strong currents prevented the collection of larger numbers of replicates. Upon recovery, the specimens were photographed and stored at –20°C.

Collection of seawater POM and DIC samples

Mixed layer suspended particulate organic matter (POM_{susp}) and dissolved inorganic carbon (DIC) in seawater was collected from three stations at each of the Gully MPA and Haddock Channel, which spatially bracket Shortland Canyon (Fig. 1). Samples were collected using a CTD/Rosette equipped with temperature, salinity and oxygen sensors, and 20 L Niskin bottles. POM_{susp} was collected by filtering seawater collected at the depth of maximum dissolved oxygen (~20 m) onto pre-combusted 70 mm QMA filters using custom stainless-steel manifolds and immediately frozen. Depth profiles of DIC were collected at nominal depths of 2, 20, 80, 125, 250, 400, 700 and 900 m, then transferred into 250 mL bottles, poisoned with 50 µL saturated HgCl₂ and stored in darkness under room temperature.

Bulk stable isotope analysis of biological tissues

Frozen tissues from each specimen were freeze-dried and homogenized with a mortar and pestle. Aliquots for $\delta^{13}\text{C}_{\text{bulk}}$ analysis were decarbonated in 10 % HCl, neutralized with de-ionized water, and re-dried at 50°C. Aliquots for $\delta^{15}\text{N}_{\text{bulk}}$ analysis were not acid treated. Analysis was conducted by Elemental Analyzer - Isotope Ratio Mass Spectrometry (EA-IRMS) at Dalhousie University. $\delta^{13}\text{C}_{\text{bulk}}$ and $\delta^{15}\text{N}_{\text{bulk}}$ are reported in δ -notation: $\delta X = [(R_{\text{sample}}/R_{\text{standard}}) - 1] \times 10^3$ where X is ^{13}C or ^{15}N and R is $^{13}\text{C}/^{12}\text{C}$ or $^{15}\text{N}/^{14}\text{N}$, respectively. Values are presented in per mil (‰) units referenced to the standards Vienna Pee Dee Belemnite (VPDB) or atmospheric

N_2 for carbon and nitrogen, respectively. Repeatability of sample replicates averaged 0.2 ‰ for both $\delta^{13}C_{bulk}$ and $\delta^{15}N_{bulk}$.

Compound-specific isotope analysis of biological tissues

Compound-specific isotope analysis was conducted at Dalhousie University following procedures in Chen et al.⁴⁴ and references therein. Aliquots of homogenized tissues were hydrolysed in 6 N HCl at 110°C for 20 h, then spiked with a norleucine internal standard and purified through cation exchange resin. Amino acids were converted to isopropyl-trifluoroacetic anhydride derivatives and analysed with co-derivatized calibration standards on a Thermo Trace 1310 GC coupled with a Delta V IRMS. Reproducibility of individual $\delta^{15}N_{AA}$ values averaged 0.5 ‰. “Glx” refers to both glutamic acid (Glu) and the glutamine converted to Glu during hydrolysis. Similarly, “Asx” refers to aspartic acid (Asp) and asparagine. Trophic position (TP) = $(\delta^{15}N_{Glx \text{ or } Ala} - \delta^{15}N_{Phe} - \beta)/TEF + 1$ was calculated following Chikaraishi et al.³⁷ with trophic enrichment factor (TEF) and β values from Decima and Landry⁴³. For TP_{met}, $\beta_{Glx} = 3.4$ and TEF_{Glx} = 6.1; for TP_{prot}, $\beta_{Ala} = 3.2$ and TEF_{Ala} = 4.5. The ΣV parameter for microbial resynthesis was calculated as $1/n \sum Abs(x_i)$, where x_i is the difference in $\delta^{15}N$ between each of the Tr-AAs (Glx, Asx, Ala, Leu, Ile, Pro, Val) and the average of those same Tr-AAs³⁹.

Preparation and analysis of seawater POM and DIC samples

DIC samples were prepared for isotopic analysis using Gas Bench IRMS methods of Torres et al.⁷⁵ for $\delta^{13}C$ measurements and headspace extraction methods of Gao et al.⁷⁶. Slight modifications to ^{14}C methods used are described in Zeidan et al.⁷⁷. POM_{susp} samples were prepared following methods of Fox and Walker⁷⁸. Briefly, they were dried at 50°C/8 h in pre-combusted (540°C/2 h) petri dishes and subsequently 12 N HCl vapour phase acidified for 4 h to remove inorganic carbon. POM samples were dried again at 50°C/8 h to remove residual HCl and H₂O vapour. Dried POM filter fractions were either pelletized for analysis of $\delta^{13}C$ and $\delta^{15}N$ via EA-IRMS at UC Santa Cruz, or closed-tube combusted for ^{14}C analysis.

Accelerator Mass Spectrometry ^{14}C analysis

One sample of decarbonated tissue from each of the biological taxa and seawater DIC and POC were analysed for natural abundance ^{14}C dating either at the André E. Lalonde National Facility using a Mini Carbon Dating System (MICADAS) or a compact 500MV NEC at the UC Irvine Keck Carbon Cycle Laboratory. CO₂ evolved from all samples were reduced to graphite via H₂ reduction or the sealed-tube Zn method^{79,80}. Results are reported in accordance with the conventions in Stuiver and Polach⁸¹. DIC $\Delta^{14}C$ data were corrected for year of sample collection with a total analytical reproducibility better than ± 2 ‰. All other $\Delta^{14}C$ measurements were corrected for year of measurement. Isotopic $\Delta^{14}C$ results are reported as Fraction Modern (Fm), $\Delta^{14}C$, and conventional radiocarbon age (ybp).

Data availability

Data is provided within the manuscript or supplementary information files.

Received: 19 April 2024; Accepted: 3 February 2025

Published online: 25 February 2025

References

- Roberts, J. M., Wheeler, A. J. & Freiwald, A. Reefs of the deep: the biology and geology of cold-water coral ecosystems. *Science* **312**, 543–547. <https://doi.org/10.1126/science.1119861> (2006).
- Beazley, L. I., Kenchington, E. L., Murillo, F. J. & Sacau, M. Deep-sea sponge groups enhance diversity and abundance of epibenthic megafauna in the Northwest Atlantic. *ICES J. Mar. Sci.* **70**, 1471–1490. <https://doi.org/10.1093/icesjms/fst124> (2013).
- Maier, S. R. et al. Reef communities associated with ‘dead’ cold-water coral framework drive resource retention and recycling in the deep sea. *Deep Res. Part. I Oceanogr. Res. Pap.* **175**, 103574. <https://doi.org/10.1016/j.dsr.2021.103574> (2021).
- Rossi, S., Coppari, M. & Viladrich, N. *Benthic-Pelagic Coupling: New Perspectives in the Animal Forests*. In: Rossi, S., (ed Bramanti, A.) Orejas Saco del Valle, C. Marine Animal Forests Springer, Cham. (2016). https://doi.org/10.1007/978-3-319-17001-5_23-1
- Cael, B. B., Dutkiewicz, S. & Henson, S. Abrupt shifts in 21st-century plankton communities. *Sci. Adv.* **7**, 1–10. <https://doi.org/10.1126/sciadv.abf8593> (2021).
- Sherwood, O. A., Guilderson, T. P., Batista, F. C., Schiff, J. T. & McCarthy, M. D. Increasing subtropical north Pacific Ocean nitrogen fixation since the little ice age. *Nature* **505**, 78–81. <https://doi.org/10.1038/nature12784> (2014).
- Ullah, H., Nagelkerken, I., Goldenberg, S. U. & Fordham, D. A. Climate change could drive marine food web collapse through altered trophic flows and cyanobacterial proliferation. *PLoS Biol.* **16**, 1–21. <https://doi.org/10.1371/journal.pbio.2003446> (2018).
- Campanyà-Llovet, N., Snelgrove, P. V. R. & Parrish, C. C. Rethinking the importance of food quality in marine benthic food webs. *Prog Oceanogr.* **156**, 240–251. <https://doi.org/10.1016/j.poccean.2017.07.006> (2017).
- Henson, S. A. et al. Uncertain response of ocean biological carbon export in a changing world. *Nat. Geosci.* **15**, 248–254. <https://doi.org/10.1038/s41561-022-00927-0> (2022).
- Griffin, S. & Druffel, E. R. M. Sources of carbon to deep-sea corals. *Radiocarbon* **31**, 533–543. <https://doi.org/10.1017/S0033822200012121> (1989).
- Ribes, M., Coma, R. & Gili, J. Heterogeneous feeding in benthic suspension feeders: the natural diet and grazing rate of the temperate gorgonian *Paramuricea clavata* (Cnidaria: Octocorallia) over a year cycle. *Mar. Ecol. Prog Ser.* **183**, 125–137. <https://doi.org/10.3354/meps183125> (1999).
- Sherwood, O. A., Jamieson, R. E., Edinger, E. N. & Wareham, V. E. Stable C and N isotopic composition of cold-water corals from the Newfoundland and Labrador continental slope: examination of trophic, depth and spatial effects. *Deep Res. Part. I Oceanogr. Res. Pap.* **55**, 1392–1402. <http://dx.doi.org/10.1016%2Fj.dsr.2008.05.013> (2008).
- Coma, R., Ribes, M., Gili, J. P. & Hughes, R. N. The ultimate opportunists: consumers of seston. *Mar. Ecol. Prog Ser.* **2019** (305–308). <https://doi.org/10.3354/meps219305> (2001).
- Orejas, C., Gili, J. M., Lopez-Gonzalez, P. J. & Arntz, W. E. Feeding strategies and diet composition of four Antarctic cnidarian species. *Polar Biol.* **24**, 620–627. <https://doi.org/10.1007/s003000100272> (2001).

15. Imbs, A. B., Demidkova, D. A. & Dautova, T. N. Lipids and fatty acids of cold-water soft corals and hydrocorals: a comparison with tropical species and implications for coral nutrition. *Mar. Biol.* **163**, 1–12. <https://doi.org/10.1371/journal.pone.0215759> (2016).
16. Rakka, M. et al. Contrasting metabolic strategies of two co-occurring deep-sea octocorals. *Sci. Rep.* **11**, 1–12. <https://doi.org/10.1038/s41598-021-90134-5> (2021).
17. Girard, F. et al. Phenology in the deep sea: seasonal and tidal feeding rhythms in a keystone octocoral. *Proc. R. Soc. B Biol. Sci.* **289**, (2022). <https://doi.org/10.1098/rspb.2022.1033>
18. Reiswig, H. M. Particle feeding in natural populations of three Marine demosponges. *Biol. Bull.* **141**, 568–591. <https://doi.org/10.2307/1540270> (1971).
19. Pile, A. J. & Young, C. M. The natural diet of a hexactinellid sponge: benthic-pelagic coupling in a deep-sea microbial food web. *Deep Res. Part. I Oceanogr. Res. Pap.* **53**, 1148–1156. <https://doi.org/10.1016/j.dsr.2006.03.008> (2006).
20. Kazanidis, G., van Oevelen, D., Veuger, B. & Witte, U. F. M. Unravelling the versatile feeding and metabolic strategies of the cold-water ecosystem engineer Spongosorites coralliophaga (Stephens, 1915). *Deep Res. Part. I Oceanogr. Res. Pap.* **141**, 71–82. <https://doi.org/10.1016/j.dsr.2018.07.009> (2018).
21. Rix, L. et al. Coral mucus fuels the sponge loop in warm-and cold-water coral reef ecosystems. *Sci. Rep.* **6**, 1–11. <https://doi.org/10.1038/srep18715> (2016).
22. Hanz, U. et al. The important role of sponges in carbon and nitrogen cycling in a deep-sea biological hotspot. *Funct. Ecol.* **36**, 2188–2199. <https://doi.org/10.1111/1365-2435.14117> (2022).
23. Vinha, B. et al. Trophic ecology of Angolan cold - water coral reefs (SE Atlantic) based on stable isotope analyses. *Sci. Rep.* 1–14. <https://doi.org/10.1038/s41598-023-37035-x> (2023).
24. van Oevelen, D. et al. Niche overlap between a cold-water coral and an associated sponge for isotopically enriched particulate food sources. *PLoS One*. **13**, 1–16. <https://doi.org/10.1371/journal.pone.0194659> (2018).
25. Reigel, A., Easson, C., Apprill, A., Freeman, C. & Bartley, M. Sponge-derived matter is assimilated by coral holobionts. *Commun. Biol.* 1–24. <https://doi.org/10.1038/s42003-024-05836-z> (2024).
26. Bart, M. C. et al. Differential processing of dissolved and particulate organic matter by deep-sea sponges and their microbial symbionts. *Sci. Rep.* **10**, 1–13. <https://doi.org/10.1038/s41598-020-74670-0> (2020).
27. Mortensen, P. B. & Buhl-Mortensen, L. Deep-water corals and their habitats in the Gully, a submarine canyon off Atlantic Canada. *Cold-Water Corals Ecosyst.* 247–277. https://doi.org/10.1007/3-540-27673-4_12 (2005).
28. Edinger, E. N. et al. Geological features supporting deep-sea coral habitat in Atlantic Canada. *Cont. Shelf Res.* **31**, 69–84. <https://doi.org/10.1016/j.csr.2010.07.004> (2011).
29. Philibert, G. et al. Updated surficial geology compilation of the Scotian Shelf bioregion, offshore Nova Scotia and New Brunswick, Canada; *Geological Survey of Canada, Open File 8911*. (2022). <https://doi.org/10.4095/330474>
30. Iken, K., Brey, T., Wand, U., Voigt, J. & Junghans, P. Food web structure of the benthic community at the Porcupine Abyssal Plain (NE Atlantic): a stable isotope analysis. *Prog. Oceanogr.* **50**, 383–405. [https://doi.org/10.1016/S0079-6611\(01\)00062-3](https://doi.org/10.1016/S0079-6611(01)00062-3) (2001).
31. Fry, B. *Stable Isotope Ecology* (Springer, 2006). <https://doi.org/10.1007/0-387-33745-8>
32. Hobson, K. A. et al. A stable isotope ($\delta^{13}\text{C}$, $\delta^{15}\text{N}$) model for the North Water food web: implications for evaluating trophodynamics and the flow of energy and contaminants. *Deep Res. Part. II Top. Stud. Oceanogr.* **49**, 5131–5150. [https://doi.org/10.1016/S0967-0645\(02\)00182-0](https://doi.org/10.1016/S0967-0645(02)00182-0) (2002).
33. Sherwood, G. D. & Rose, G. A. Stable isotope analysis of some representative fish and invertebrates of the Newfoundland and Labrador continental shelf food web. *Estuar. Coast Shelf Sci.* **63**, 537–549. <https://doi.org/10.1016/j.ecss.2004.12.010> (2005).
34. Newsome, S. D., Carlos, M. R., Bearhop, S. & Phillips, D. L. A niche for isotopic ecology. *Front. Ecol. Environ.* <https://doi.org/10.1890/060150.1> (2007).
35. Ohkouchi, N. et al. Advances in the application of amino acid nitrogen isotopic analysis in ecological and biogeochemical studies. *Org. Geochem.* **113**, 150–174. <https://doi.org/10.1016/j.orggeochem.2017.07.009> (2017).
36. McClelland, J. W. & Montoya, J. P. Trophic relationships and the Nitrogen Isotopic composition of amino acids in Plankton. *Ecology* **83**, 2173–2180. [https://doi.org/10.1890/0012-9658\(2002\)083](https://doi.org/10.1890/0012-9658(2002)083) (2002). [2173:TRATNI]2.0.CO;2.
37. Chikaraishi, Y. et al. Determination of aquatic food-web structure based on compound-specific nitrogen isotopic composition of amino acids. *Limnol. Oceanogr. Methods*. **7**, 740–750. <https://doi.org/10.4319/lom.2009.7.740> (2009).
38. McMahon, K. W. & McCarthy, M. D. Embracing variability in amino acid $\delta^{15}\text{N}$ fractionation: mechanisms, implications, and applications for trophic ecology. *Ecosphere* **7**, 1–26. <https://doi.org/10.1002/ecs2.1511> (2016).
39. McCarthy, M. D., Benner, R., Lee, C. & Fogel, M. L. Amino acid nitrogen isotopic fractionation patterns as indicators of heterotrophy in plankton, particulate, and dissolved organic matter. *Geochim. Cosmochim. Acta*. **71**, 4727–4744. <https://doi.org/10.1016/j.gca.2007.06.061> (2007).
40. Hannides, C. C. S., Popp, B. N., Choy, A., Drazen, J. C. & C. & Midwater zooplankton and suspended particle dynamics in the North Pacific Subtropical Gyre: a stable isotope perspective. *Limnol. Oceanogr.* **58**, 1931–1946. <https://doi.org/10.4319/lo.2013.58.6.1931> (2013).
41. Yamaguchi, Y. T. & McCarthy, M. D. Sources and transformation of dissolved and particulate organic nitrogen in the North Pacific Subtropical Gyre indicated by compound-specific $\delta^{15}\text{N}$ analysis of amino acids. *Geochim. Cosmochim. Acta*. **220**, 329–347. <https://doi.org/10.1016/j.gca.2017.07.036> (2018).
42. Sherwood, O. A., Lehmann, M. F., Schubert, C. J., Scott, D. B. & McCarthy, M. D. Nutrient regime shift in the western North Atlantic indicated by compound-specific $\delta^{15}\text{N}$ of deep-sea gorgonian corals. *Proc. Natl. Acad. Sci. U. S. A.* **108**, 1011–1015. (2011). <https://doi.org/10.1073/pnas.1004904108>
43. Décima, M. & Landry, M. R. Resilience of plankton trophic structure to an eddy-stimulated diatom bloom in the north pacific subtropical gyre. *Mar. Ecol. Prog. Ser.* **643**, 33–48. <https://doi.org/10.3354/meps13333> (2020).
44. Chen, S. M., Mudie, P. & Sherwood, O. A. Amino acid $\delta^{13}\text{C}$ and $\delta^{15}\text{N}$ fingerprinting of sea ice and pelagic algae in Canadian Arctic and Subarctic seas. *Front. Mar. Sci.* **9**, 1–16. <https://doi.org/10.3389/fmars.2022.976908> (2022).
45. Wojtal, P. K. et al. Deconvolving mechanisms of particle flux attenuation using nitrogen isotope analyses of amino acids. *Limnol. Oceanogr.* **68**, 1965–1981. <https://doi.org/10.1002/lno.12398> (2023).
46. Bauer, J. E., Druffel, E. R. M., Wolgast, D. M. & Griffin, S. Temporal and regional variability in sources and cycling of DOC and POC in the northwest Atlantic continental shelf and slope. *Deep Res. Part. II Top. Stud. Oceanogr.* **49**, 4387–4419. [https://doi.org/10.1016/S0967-0645\(02\)00123-6](https://doi.org/10.1016/S0967-0645(02)00123-6) (2002).
47. Thomsen, L. et al. The Oceanic Biological pump: Rapid carbon transfer to depth at Continental Margins during Winter. *Sci. Rep.* **7**, 1–10. <https://doi.org/10.1038/s41598-017-11075-6> (2017).
48. DeVries, T. The Ocean Carbon Cycle. *Annu. Rev. Environ. Resour.* **47**, 317–341. <https://doi.org/10.1146/annurev-environ-120920-111307> (2022).
49. Liu, Q. et al. Reinterpreting radiocarbon records in bamboo corals – new insights from the tropical North Atlantic. *Geochim. Cosmochim. Acta*. **348**, 296–308. <https://doi.org/10.1016/j.gca.2023.03.019> (2023).
50. Mortensen, P. B. & Buhl-Mortensen, L. Morphology and growth of the deep-water gorgonians *Primnoa resedaeformis* and *Paragorgia arborea*. *Mar. Biol.* **147**, 775–788. <https://doi.org/10.1007/s00227-005-1604-y> (2005).

51. Johanson, A. N., Flögel, S., Dullo, W. C., Linke, P. & Hasselbring, W. Modeling polyp activity of *Paragorgia arborea* using supervised learning. *Ecol. Inf.* **39**, 109–118. <https://doi.org/10.1016/j.ecoinf.2017.02.007> (2017).
52. Dai, C. F. & Lin, M. C. The effects of flow on feeding of three gorgonians from southern Taiwan. *J. Exp. Mar. Bio Ecol.* **173**, 57–69. [https://doi.org/10.1016/0022-0981\(93\)90207-5](https://doi.org/10.1016/0022-0981(93)90207-5) (1993).
53. Lacharité, M. & Metaxas, A. Early life history of deep-water gorgonian corals may limit their abundance. *PLoS One*. **8**, e65394. <https://doi.org/10.1371/journal.pone.0065394> (2013).
54. Orejas, C. et al. The effect of flow speed and food size on the capture efficiency and feeding behaviour of the cold-water coral *Lophelia pertusa*. *J. Exp. Mar. Bio Ecol.* **481**, 34–40. <https://doi.org/10.1016/j.jembe.2016.04.002> (2016).
55. Huvenne, V. A. I. et al. A picture on a wall: innovative mapping reveals cold-water coral refuge in submarine canyon. In J. M. Roberts (Ed.), *PLoS ONE*. **6**, e28755. Public Library of Science (PLoS). (2011). <https://doi.org/10.1371/journal.pone.0028755>
56. Robert, K., Jones, D. O. B., Georgiopoulou, A. & Huvenne, V. A. I. Cold-water coral assemblages on vertical walls from the northeast Atlantic. *Divers. Distrib.* **26** (3), 284–298. <https://doi.org/10.1111/ddi.13011> (2019).
57. Lampitt, R. S. & Paterson, G. L. J. The feeding behaviour of an abyssal sea anemone from in situ time lapse photographs and trawl samples. *Oceanol. Acta*. **10**, 455–461 (1987).
58. Sebens, K. P. & Koehl, M. A. R. Predation on zooplankton by the benthic anthozoans *Alcyonium Siderium* (Alcyonacea) and *Metridium senile* (Actiniaria) in the New England subtidal. *Mar. Biol.* **81**, 255–271. <https://doi.org/10.1007/BF00393220> (1984).
59. Gilkinson, K. & Edinger, E. The Ecology of deep-sea Corals of Newfoundland and Labrador Waters. *Canadian Technical Report of Fisheries and Aquatic Sciences* No. 2830. 136 (2009).
60. Sun, J., Hamel, J. F., Shikon, V., Cossignani, E. F. & Mercier, A. Trophic ecology, diet and feeding behaviour of three bathyal sea anemones (Actiniaria: Cnidaria) in the Northwest Atlantic. *Deep Res. Part. I Oceanogr. Res. Pap.* 179. <https://doi.org/10.1016/j.dsr.2021.103678> (2022).
61. de Goeij, J. M., Lesser, M. P. & Pawlik, J. R. Nutrient fluxes and ecological functions of coral reef sponges in a changing ocean. in *Climate Change, Ocean Acidification and Sponges: Impacts Across Multiple Levels of Organization* 373–410. (2017). https://doi.org/10.1007/978-3-319-59008-0_8
62. Pawlik, J. R. & McMurray, S. E. The Emerging Ecological and Biogeochemical Importance of sponges on Coral Reefs. *Ann. Rev. Mar. Sci.* **12**, 315–337. <https://doi.org/10.1146/annurev-marine-010419-010807> (2019).
63. Kahn, A. S., Chu, J. W. F. & Leys, S. P. Trophic ecology of glass sponge reefs in the Strait of Georgia, British Columbia. *Sci. Rep.* **8**, 1–11. <https://doi.org/10.1038/s41598-017-19107-x> (2018).
64. Polunin, N. V. C., Pawsey, W. E., Cartes, J. E., Pinnegar, J. K. & Moranta, J. Feeding relationships in Mediterranean bathyal assemblages elucidated by stable nitrogen and carbon isotope data. *Mar. Ecol. Prog Ser.* **220**, 13–23. <https://doi.org/10.3354/meps220013> (2001).
65. Matich, P., Bizzarro, J. J. & Shipley, O. N. Are stable isotope ratios suitable for describing niche partitioning and individual specialization? *Ecol. Appl.* **31**, 1–8. <https://doi.org/10.1002/eap.2392> (2021).
66. Breeze, H., Davis, D. S., Butler, M. & Kostylev, V. Distribution and status of deep sea corals off Nova Scotia. Marine Issues Committee Special Publication No 1, Ecology Action Centre, Halifax, NS. (1997).
67. Wareham, V. E. & Edinger, E. N. Distribution of deep-sea corals in the Newfoundland and Labrador region, Northwest Atlantic Ocean. *Bull. Mar. Sci.* **81**, 289–313. (2007).
68. Gullage, L., Devillers, R. & Edinger, E. N. Predictive distribution modelling of cold-water corals in the Newfoundland and Labrador region. *Mar. Ecol. Prog Ser.* **582**, 57–77. <https://doi.org/10.3354/meps12307> (2017).
69. Packer et al. State of deep-sea coral and sponge ecosystems of the northeastern United States. In: Hourigan TF, Etnoyer PJ, Cairns SD (eds.). *The State of Deep-Sea Coral and Sponge Ecosystems of the United States*. NOAA Technical Memorandum NMFS-OHC-4. Silver Spring, MD. 61. (2021).
70. Beazley, L., Lirette, C. & Guizarro, J. Characterization of the Corals and Sponges of the Eastern Scotian Slope from a Benthic Imagery Survey. *Canadian technical report of Fisheries and Aquatic Sciences* 3302. 91p. (2017).
71. Brooke, S. et al. Distributions and habitat associations of deep water corals in Norfolk and Baltimore canyons of the Mid-atlantic Bight, USA. *Deep Sea Res.* **137**, 131–147 (2017).
72. McMahon, K. W., McCarthy, M. D., Sherwood, O. A., Larsen, T. & Guilderson, T. P. Millennial-scale plankton regime shifts in the subtropical North Pacific Ocean. *Science* **350**, 1530–1533. <https://doi.org/10.1126/science.aaa9942> (2015).
73. De Goeij, J. M. et al. Surviving in a marine desert: the sponge loop retains resources within coral reefs. *Science* **342**, 108–110. <https://doi.org/10.1126/science.1241981> (2013).
74. Bart, M. C., Hudspeth, M., Rapp, H. T., Verdonschot, P. F. M. & de Goeij, J. A deep-sea sponge loop? Sponges transfer dissolved and particulate organic carbon and nitrogen to associated fauna. *Front. Mar. Sci.* **8**. <https://doi.org/10.3389/fmars.2021.604879> (2021).
75. Torres, M. E., Mix, A. C. & Rugh, W. D. Precise $\delta^{13}\text{C}$ analysis of dissolved inorganic carbon in natural waters using automated headspace sampling and continuous-flow mass spectrometry. *Limnol. Oceanogr. Methods.* **3**, 349–360. <https://doi.org/10.4319/lom.2005.3.349> (2005).
76. Gao, P. et al. Rapid sample preparation of dissolved inorganic carbon in natural waters using a headspace-extraction approach for radiocarbon analysis by accelerator mass spectrometry. *Limnol. Oceanogr. Methods.* **12**, 174–190. <https://doi.org/10.4319/lom.2014.12.174> (2014).
77. Zeidan, S. et al. Using Radiocarbon measurements of dissolved Inorganic Carbon to determine a revised Residence Time for Deep Baffin Bay. *Front. Mar. Sci.* **9**, 1–14. <https://doi.org/10.3389/fmars.2022.845536> (2022).
78. Fox, A. & Walker, B. D. Sources and Cycling of Particulate Organic Matter in Baffin Bay: a multi-isotope $\delta^{13}\text{C}$, $\delta^{15}\text{N}$, and $\Delta^{14}\text{C}$ Approach. *Front. Mar. Sci.* **9**, 1–14. <https://doi.org/10.3389/fmars.2022.846025> (2022).
79. Vogel, J. S., Southon, J. R. & Nelson, D. E. Catalyst and binder effects in the use of filamentous graphite for AMS. *Nucl. Inst. Methods Phys. Res. B.* **29**, 50–56. [https://doi.org/10.1016/0168-583X\(87\)90202-3](https://doi.org/10.1016/0168-583X(87)90202-3) (1987).
80. Walker, B. D. & Xu, X. An improved method for the sealed-tube zinc graphitization of microgram carbon samples and ^{14}C AMS measurement. *Nucl. Instruments Methods Phys. Res. Sect. B Beam Interact. Mater. Atoms.* **438**, 58–65. <https://doi.org/10.1016/j.nimb.2018.08.004> (2019).
81. Stuiver, M. & Polach, H. A. Discussion reporting of ^{14}C data. *Radiocarbon* **19**, 355–363. <https://doi.org/10.1017/S0033822200003672> (1977).

Acknowledgements

We thank MEOPAR, Atlantic Towing, Oceaneering, UTEC, DFO-NL (MCT), the officers and crew of the M/V *Atlantic Condor*, Chris Algar, Jeshua Becker, Laura Broom, Subhadeep Rakshit, and Sanjana Varanasi for a successful oceanographic expedition; Claire Normandeau for bulk stable isotope analysis; and Jennifer Walker for radiocarbon analyses. Funding was provided by a Fisheries and Oceans Canada grant to OS (10-22-24-MT-MCT-007), an NSERC ship time grant to OS et al. (RGPST-567197-2002), NSERC grants to BW (RGPIN2020-06501, RGPAS-2020-00071, DGEGR-2020-00256) and the Canada Research Chairs program to BW (CRC-2018-00050).

Author contributions

OS and BN collected specimens. FJM completed taxonomic identification of specimens. WG conducted bulk and compound specific isotopic analyses. LJ, AF and BW conducted radiocarbon analyses of DIC and POM samples. WG and OS wrote the manuscript. FJM, BN, EK, BW, and EE provided comments on the original manuscript. All authors reviewed the manuscript.

Declarations

Competing interests

The authors declare no competing interests.

Additional information

Supplementary Information The online version contains supplementary material available at <https://doi.org/10.1038/s41598-025-89116-8>.

Correspondence and requests for materials should be addressed to W.G.

Reprints and permissions information is available at www.nature.com/reprints.

Publisher's note Springer Nature remains neutral with regard to jurisdictional claims in published maps and institutional affiliations.

Open Access This article is licensed under a Creative Commons Attribution-NonCommercial-NoDerivatives 4.0 International License, which permits any non-commercial use, sharing, distribution and reproduction in any medium or format, as long as you give appropriate credit to the original author(s) and the source, provide a link to the Creative Commons licence, and indicate if you modified the licensed material. You do not have permission under this licence to share adapted material derived from this article or parts of it. The images or other third party material in this article are included in the article's Creative Commons licence, unless indicated otherwise in a credit line to the material. If material is not included in the article's Creative Commons licence and your intended use is not permitted by statutory regulation or exceeds the permitted use, you will need to obtain permission directly from the copyright holder. To view a copy of this licence, visit <http://creativecommons.org/licenses/by-nc-nd/4.0/>.

© The Author(s) 2025